

A STABILISED FINITE ELEMENT METHOD FOR A FICTITIOUS DOMAIN PROBLEM ALLOWING SMALL INCLUSIONS

GABRIEL R. BARRENECHEA AND CHEHERAZADA GONZÁLEZ

ABSTRACT. The purpose of this work is to approximate numerically an elliptic partial differential equation posed on domains with small perforations (or inclusions). The approach is based on the fictitious domain method, and since the method's interest lies in the case in which the geometrical features are not resolved by the mesh, we propose a stabilised finite element method. The stabilisation term is a simple, non-consistent penalisation, that can be linked to the Barbosa-Hughes approach. Stability and optimal convergence are proved, and numerical results confirm the theory.

June 27, 2017

1. INTRODUCTION

This work is devoted to the finite element approximation of elliptic problems in domains containing small perforations. More precisely, our interest is to approximate an elliptic partial differential equation posed on the domain $\omega := \Omega \setminus \cup_{i=1}^N B_i$ where $\Omega \subset \mathbb{R}^2$ is a polygonal open domain, and $N \in \mathbb{N}$. Each B_i is a closed simply connected domain that can be, a priori, of any shape and size (see Figure 1 for a typical case). We also denote γ_i the boundary of B_i . The problem of interest reads as follows: Find $\tilde{u} : \omega \rightarrow \mathbb{R}$ such that

$$(1.1) \quad \begin{cases} -\Delta \tilde{u} = \tilde{f} & \text{in } \omega, \\ \tilde{u} = g_i & \text{on } \gamma_i, \quad i = 1, \dots, N, \\ \tilde{u} = 0 & \text{on } \partial\Omega, \end{cases}$$

where $\tilde{f} \in L^2(\omega)$ and $g_i \in H^{\frac{1}{2}}(\gamma_i)$ for all $i = 1, \dots, N$. The restriction to Dirichlet boundary conditions is of importance, and, another type of boundary conditions, e.g., Neumann boundary conditions, would lead to a different approach. Nevertheless, our motivation is to use a method like the one proposed in this work to approximate a problem like (1.1), but in incompressible fluid mechanics, i.e., solving a Stokes, or even Navier-Stokes, equation. In such a case, Dirichlet conditions posed on each one of the perforations are the typical ones.

1991 *Mathematics Subject Classification.* 65M85, 65N15, 65N30.

Key words and phrases. fictitious domain; stabilised method; small geometrical features.

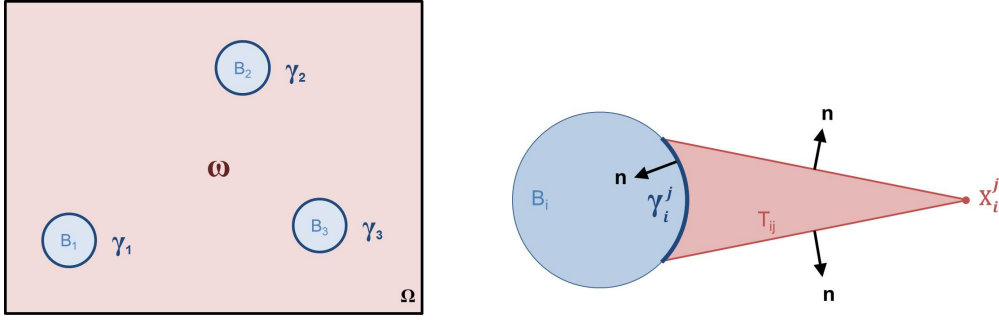


FIGURE 1. Physical domain ω , fictitious domain Ω and inclusions B_i (left). On the right, the curved triangle T_{ij} used in the proof of Lemma 3.1.

We now present some notation that will be used on what follows. We adopt the standard notation for Sobolev spaces (aligned with, e.g., [10]). In particular, for $D \subseteq \mathbb{R}^2$, $H^1(D)$ ($H_0^1(D)$) will denote the space of (generalised) functions of $L^2(D)$ with first derivatives also belonging to $L^2(D)$ (and that vanish on ∂D). The inner product on $L^2(D)$ is denoted by $(\cdot, \cdot)_D$, its associated norm is denoted by $\|\cdot\|_{0,D}$, and the norm (seminorm) in $H^1(D)$ is denoted by $\|\cdot\|_{1,\Omega}$ ($|\cdot|_{1,\Omega}$). We keep the same notation for vector-valued functions. The space of traces of functions of $H^1(D)$ on ∂D is denoted by $H^{\frac{1}{2}}(\partial D)$, its dual with respect to the $L^2(\partial D)$ inner product is denoted by $H^{-\frac{1}{2}}(\partial D)$, and the duality pairing between them is denoted by $\langle \cdot, \cdot \rangle_{\partial D}$. Their norms are denoted by $\|\cdot\|_{-\frac{1}{2},\partial D}$ and $\|\cdot\|_{\frac{1}{2},\partial D}$, respectively.

In this work we follow the approach described in [13] for fictitious domain methods (the description in that work is for a problem posed in a slightly simpler situation than the one described here, but the extension of their results to our situation is straightforward): we first introduce an extension f of \tilde{f} to Ω , and state the following mixed problem: Find $(u, \boldsymbol{\lambda}) \in W := H_0^1(\Omega) \times \Pi_{i=1}^N H^{-\frac{1}{2}}(\gamma_i)$, where $\boldsymbol{\lambda} = (\lambda_i)_{i=1}^N$, such that

$$(1.2) \quad \begin{aligned} (\nabla u, \nabla v)_\Omega - \sum_{i=1}^N \langle \lambda_i, v \rangle_{\gamma_i} &= (f, v)_\Omega, \\ \sum_{i=1}^N \langle \mu_i, u \rangle_{\gamma_i} &= \sum_{i=1}^N \langle \mu_i, g_i \rangle_{\gamma_i}, \end{aligned}$$

for all $(v, \boldsymbol{\mu}) \in W$, $\boldsymbol{\mu} = (\mu_i)_{i=1}^N$. This weak problem was proposed as an approximation of (1.1) in [14], and the method was later analysed in [13]. In fact, (1.2) is proven to be well-posed in [13], and it is linked to (1.1) as follows: if $(u, \boldsymbol{\lambda})$ satisfies (1.2), then $u|_\omega$ satisfies (1.1), and the Lagrange multipliers λ_i satisfy $\lambda_i = \llbracket \partial_{\mathbf{n}} u \rrbracket_{\gamma_i}$, for $i = 1, \dots, N$, where $\llbracket v \rrbracket_{\gamma_i}$ stands for the jump of a function v across γ_i (see [13] for details).

To discretise (1.2), we introduce \mathcal{T}_h , a regular triangulation of $\bar{\Omega}$ built using triangles K with diameter h_K , and $h := \max_{K \in \mathcal{T}_h} h_K$. Additionally, each γ_i is partitioned into a different mesh $\gamma_{i,\tilde{h}}$ with curved edges \tilde{e} , where $\tilde{h} := \max |\tilde{e}|$. Associated to these partitions, we define the

following finite element spaces:

$$\begin{aligned} V_h &= \{v_h \in C^0(\bar{\Omega}) : v_h|_K \in \mathbb{P}_1(K), \forall K \in \mathcal{T}_h\}, \\ \Lambda_{i,\tilde{h}} &= \{\mu_{\tilde{h}} \in L^2(\gamma_i) : \mu_{\tilde{h}}|_{\tilde{e}} \in \mathbb{P}_0(\tilde{e}), \forall \tilde{e} \in \gamma_{i,\tilde{h}}\} \quad \text{for } i = 1, \dots, N, \\ \mathbf{\Lambda}_{\tilde{h}} &= \prod_{i=1}^N \Lambda_{i,\tilde{h}}. \end{aligned}$$

The order of the finite element spaces is the same one as in [13]. As a matter of fact, most, if not all, the work in fictitious domain approaches focuses in low-order approximations. This is due to the fact that, even in the case ω is a smooth domain, then the solution of (1.2) is not smooth. In fact, each λ_i belongs, at least, to $L^2(\gamma_i)$, but in general we only have $u \in H^{\frac{3}{2}-\epsilon}(\Omega)$, for any $\epsilon > 0$, unless the extension f is chosen very carefully, (see [13] for a discussion on this, and the recent work [11] for some recent results on how to circumvent this problem using an optimization approach). In the original paper [13] the pair $V_h \times \mathbf{\Lambda}_{\tilde{h}}$ was proven to be inf-sup stable only if $|\tilde{e}| \geq 3h$, for every edge \tilde{e} in every $\gamma_{i,\tilde{h}}$. This condition is not only sufficient, but also necessary for stability (see [3] for a numerical experiment confirming this fact). Then, in [3] a local projection inspired method was proposed to circumvent this restriction. The first step of the latter method was to identify an inf-sup stable subspace of $\mathbf{\Lambda}_{\tilde{h}}$, and project the discrete Lagrange multipliers onto it. Then, even if the restriction on the meshes was not necessary for the stability and convergence, at least the existence of a macro-mesh that satisfied it was needed. Other approaches have also been proposed in the recent years to avoid this restriction, such as using cut elements as in, for instance, [5, 6], XFEM approaches as in [20, 16], the *fat boundary method* [19, 4], or non-boundary fitted meshes (see, e.g., [22]).

This work focuses on perforated domains, i.e., domains with holes (or inclusions) that are smaller than the characteristic mesh width. In our case, this amounts to stating that $\text{diam}(B_i) \ll \text{diam}(\Omega)$, and in turn, this will imply that, in most cases, $|\tilde{e}| < h$, which is precisely the case not allowed in [13]. Over the years many authors have proposed solutions to this problem. One alternative is the Composite FEM method, see, e.g., [15], where the geometrical features are included in the finite element space, thus proposing a method whose dimension does not necessarily depend on the number of geometrical inclusions, see also [21] for the application of the same idea to the Stokes problem, and [12] for an adaptive strategy associated to a discontinuous Galerkin version of this method. Alternatively, the geometrical features of the domain can be taken into account at the mesh generation step. This idea is at the basis of some recent developments on discontinuous Galerkin methods on general polyhedral meshes (see [7], and [1] for a recent review). Finally, it is interesting to mention the approach described in [18] (see also the references therein for an extensive review of this type of approach), where a multiscale problem on a domain with inclusions has been approximated using a multiscale finite element approach based on the enrichment of the Crouzeix-Raviart method with bubble functions.

The purpose of this work is to propose a simple alternative to the above-mentioned approaches. As we stated before, each one of the Lagrange multipliers satisfies $\lambda_i = \llbracket \partial_n u \rrbracket_{\gamma_i}$. Then, a natural idea is to penalise the difference between the two, adding a least-squares term, very linked to the method of Barbosa and Hughes (see [2], also applied in the context of fictitious domains in combination with an XFEM approach in [16]). This idea, although natural, leads to technical difficulties on the error analysis of the resulting method (see Remark 3.3 below for a discussion). Then, we propose a simpler presentation leading to a non-consistent method, but whose error can be proven to be of optimal order. This simpler alternative is also easier to implement, and modifies only one of the blocks of the finite element matrix, thus avoiding any extra couplings between the unknowns. Also, it is worth mentioning that since the finite element spaces for u and

λ are independent considering a larger space $\Lambda_{\bar{h}}$ is allowed. This provides a better (although, still weak) imposition of the boundary condition $u = g_i$ on each γ_i .

The rest of this manuscript is organised as follows. In Section 2 we present the method, and prove its stability. The error analysis is presented in Section 3, some numerical results are presented in Section 4, and some conclusions are finally drawn.

2. THE STABILISED FORMULATION AND ITS STABILITY

We now propose the stabilised Finite Element method considered in this work: Find $(u_h, \lambda_{\bar{h}}) \in W_h := V_h \times \Lambda_{\bar{h}}$ such that

$$(2.1) \quad \mathbf{B}((u_h, \lambda_{\bar{h}}), (v_h, \mu_{\bar{h}})) = (f, v_h)_\Omega - \sum_{i=1}^N \langle \mu_{i, \bar{h}}, g_i \rangle_{\gamma_i} \quad \forall (v_h, \mu_{\bar{h}}) \in W_h,$$

where

$$\mathbf{B}((u_h, \lambda_{\bar{h}}), (v_h, \mu_{\bar{h}})) = (\nabla u_h, \nabla v_h)_\Omega - \sum_{i=1}^N \langle \lambda_{i, \bar{h}}, v_h \rangle_{\gamma_i} - \sum_{i=1}^N \langle \mu_{i, \bar{h}}, u_h \rangle_{\gamma_i} - \sum_{i=1}^N h \langle \lambda_{i, \bar{h}}, \mu_{i, \bar{h}} \rangle_{\gamma_i}.$$

We define the following norm

$$\|(v_h, \mu_{\bar{h}})\|_{W_h}^2 := |v_h|_{1, \Omega}^2 + \sum_{i=1}^N h \|\mu_{i, \bar{h}}\|_{0, \gamma_i}^2,$$

and prove next the stability of the method, whose proof follows directly using the definition of the bilinear form \mathbf{B} .

Theorem 2.1. *For all $(v_h, \mu_{\bar{h}}) \in W_h$, the following holds*

$$\mathbf{B}((v_h, \mu_{\bar{h}}), (v_h, -\mu_{\bar{h}})) = \|(v_h, \mu_{\bar{h}})\|_{W_h}^2.$$

Then, problem (2.1) is well-posed.

The next result states the consistency of the method for smooth solutions.

Lemma 2.1. *Let (u, λ) be the solution of (1.2) and $(u_h, \lambda_{\bar{h}}) \in W_h$ be the solution of (2.1). Then*

$$(2.2) \quad \mathbf{B}((u - u_h, \lambda - \lambda_{\bar{h}}), (v_h, \mu_{\bar{h}})) = - \sum_{i=1}^N h \langle \lambda_i, \mu_{i, \bar{h}} \rangle_{\gamma_i},$$

for all $(v_h, \mu_{\bar{h}}) \in W_h$. Moreover, if $u \in H^{\frac{3}{2} + \epsilon}(\Omega)$ for some $\epsilon > 0$, then

$$(2.3) \quad \mathbf{B}((u - u_h, \lambda - \lambda_{\bar{h}}), (v_h, \mu_{\bar{h}})) = 0 \quad \forall (v_h, \mu_{\bar{h}}) \in W_h.$$

Proof. From the definition of \mathbf{B} , and the fact that (u, λ) solves (1.2) and $(u_h, \lambda_{\bar{h}})$ solves (2.1), it follows that

$$\begin{aligned} \mathbf{B}((u, \lambda), (v_h, \mu_{\bar{h}})) &= (\nabla u, \nabla v_h)_\Omega - \sum_{i=1}^N \langle \lambda_i, v_h \rangle_{\gamma_i} - \sum_{i=1}^N \langle \mu_{i, \bar{h}}, u \rangle_{\gamma_i} - \sum_{i=1}^N h \langle \lambda_i, \mu_{i, \bar{h}} \rangle_{\gamma_i} \\ &= (f, v_h)_\Omega - \sum_{i=1}^N \langle \mu_{i, \bar{h}}, g_i \rangle_{\gamma_i} - \sum_{i=1}^N h \langle \lambda_i, \mu_{i, \bar{h}} \rangle_{\gamma_i} \\ &= \mathbf{B}((u_h, \lambda_{\bar{h}}), (v_h, \mu_{\bar{h}})) - \sum_{i=1}^N h \langle \lambda_i, \mu_{i, \bar{h}} \rangle_{\gamma_i}, \end{aligned}$$

which proves (2.2). Now, if $u \in H^{\frac{3}{2}+\epsilon}(\Omega)$, then $\lambda_i = \llbracket \partial_{\mathbf{n}} u \rrbracket_{\gamma_i} = 0$, for $i = 1, \dots, N$, and (2.3) follows from (2.2). \square

3. ERROR ANALYSIS

We start this section by making various assumptions on the meshes and inclusions. First, we will suppose that the inclusions B_i satisfy $\text{dist}(B_i, \partial\Omega) \geq h/2$. This assumption will be needed on what follows, and, although it may seem restrictive, the factor $1/2$ can be relaxed to any positive constant, as long as it is fixed. We will also need to include an indicator of how "clustered" the inclusions are. For this we start defining, for every $i = 1, \dots, N$, the local annular neighborhood \tilde{B}_i by

$$(3.1) \quad \tilde{B}_i := \{\mathbf{x} \in \omega : \text{dist}(\mathbf{x}, \gamma_i) \leq h/2\},$$

and make the following assumption: There exists a constant $M > 0$, independent of h and $\text{diam}(B_i)$, such that

$$(3.2) \quad \#\{\tilde{B}_i : \tilde{B}_i \cap K\} \leq M \quad \forall K \in \mathcal{T}_h.$$

We will finally assume, just to simplify the presentation, that the inclusions B_i are convex. This latter hypothesis is made only for simplicity, the same results are valid, up to minor modifications, if this does not hold.

We start the error analysis by stating the following local trace inequality. The proof of this result is similar to the one given in [8] for the case of curved elements.

Lemma 3.1. *Let \tilde{B}_i be the neighbourhood defined in (3.1). Then, for every $v \in H^1(\Omega)$, the following local trace inequality holds*

$$(3.3) \quad \|v\|_{0,\gamma_i}^2 \leq 8 \left(h^{-1} \|v\|_{0,\tilde{B}_i}^2 + \|v\|_{0,\tilde{B}_i} \|\nabla v\|_{0,\tilde{B}_i} \right).$$

Proof. Let $v \in H^1(\Omega)$. We split $\gamma_i = \cup_{j=1}^R \overline{\gamma_i^j}$, where the γ_i^j are disjoint, and introduce a collection of points $\mathbf{x}_i^j \in \Omega \setminus B_i$ (see Figure 1) such that

$$(3.4) \quad \text{dist}(\mathbf{x}_i^j, \gamma_i^j) = \frac{1}{2}h \quad \text{and} \quad (\mathbf{x} - \mathbf{x}_i^j) \cdot \mathbf{n}|_{\gamma_i} \geq \frac{1}{4}h,$$

for all $\mathbf{x} \in \gamma_i^j$. Using these points, we build the curved triangle T_{ij} as depicted in Figure 1 (right). Let $\mathbf{m}(\mathbf{x}) = \mathbf{x} - \mathbf{x}_i^j$. In addition, we choose R (the number of subdivisions of γ_i) large enough so $\|\mathbf{m}\|_{\infty, T_{ij}} \leq h$. Then $\nabla \cdot \mathbf{m} = 2$, and $\mathbf{m} \cdot \mathbf{n} = 0$ on $\partial T_{ij} \setminus \gamma_i^j$, and Green's Theorem yields

$$(\mathbf{m} \cdot \mathbf{n}, v^2)_{\gamma_i^j} = (\mathbf{m} \cdot \mathbf{n}, v^2)_{\partial T_{ij}} = (\nabla \cdot (v^2 \mathbf{m}), 1)_{T_{ij}} = 2\|v\|_{0, T_{ij}}^2 + 2(v, \nabla v \cdot \mathbf{m})_{T_{ij}}.$$

On the other hand, from (3.4) we have $\mathbf{m} \cdot \mathbf{n}|_{\gamma_i^j} \geq \frac{1}{4}h$. Then, applying Hölder's inequality to the last expression, and the fact that $\|\mathbf{m}\|_{\infty, T_{ij}} \leq h$, we arrive at

$$\frac{1}{4}h \|v\|_{0, \gamma_i^j}^2 \leq (\mathbf{m} \cdot \mathbf{n}, v^2)_{\gamma_i^j} \leq 2\|v\|_{0, T_{ij}}^2 + 2h \|v\|_{0, T_{ij}} \|\nabla v\|_{0, T_{ij}}.$$

Then, for each γ_i^j the following holds

$$\|v\|_{0, \gamma_i^j}^2 \leq 8h^{-1} \|v\|_{0, T_{ij}}^2 + 8\|v\|_{0, T_{ij}} \|\nabla v\|_{0, T_{ij}}.$$

Hence, adding over $j = 1, \dots, R$, using that the curved triangles T_{ij} are disjoint, $\tilde{B}_i \supset \cup_{j=1}^R T_{ij}$, and applying Cauchy-Schwarz's inequality we obtain

$$\|v\|_{0,\gamma_i}^2 = \sum_{j=1}^R \|v\|_{0,\gamma_i^j}^2 \leq 8h^{-1} \sum_{j=1}^R \|v\|_{0,T_{ij}}^2 + 8 \sum_{j=1}^R \|v\|_{0,T_{ij}} \|\nabla v\|_{0,T_{ij}} \leq 8h^{-1} \|v\|_{0,\tilde{B}_i}^2 + 8 \|v\|_{0,\tilde{B}_i} \|\nabla v\|_{0,\tilde{B}_i}.$$

This finishes the proof. \square

In order to prove the error estimate, we split the error into interpolation and discrete errors as follows:

$$(e^u, e^\lambda) := (u - u_h, \lambda - \lambda_{\tilde{h}}) = (u - i_h u, \lambda - \Pi_{\tilde{h}} \lambda) + (i_h u - u_h, \Pi_{\tilde{h}} \lambda - \lambda_{\tilde{h}}) =: (\eta^u, \eta^\lambda) - (e_h^u, e_h^\lambda).$$

Here, $i_h : C^0(\bar{\Omega}) \rightarrow V_h$ stands for the Lagrange interpolation operator, and $\Pi_{\tilde{h}} \lambda \in \Lambda_{i,\tilde{h}}$ is defined by $\Pi_{\tilde{h}} \lambda = (\Pi_{\tilde{h}} \lambda_i)_{i=1}^N$ where $\Pi_{\tilde{h}} \lambda_i|_{\tilde{e}} := |\tilde{e}|^{-1}(\lambda_i, 1)_{\tilde{e}}$ for all $\tilde{e} \in \gamma_{i,\tilde{h}}$, and all $i = 1, \dots, N$. We now state the main error estimate for the method (2.1).

Theorem 3.1. *Let us suppose that $u \in H^{1+s}(\Omega)$, for $s \in (0, 1]$, and $\lambda \in \prod_{i=1}^N H^\delta(\gamma_i)$, for $\delta \in [0, \frac{1}{2}]$. Then, there exists a constant $C > 0$, independent of h and \tilde{h} , such that*

$$(3.5) \quad \|(e^u, e^\lambda)\|_{W_h} \leq C \left((1 + \sqrt{M}) h^s |u|_{1+s,\Omega} + h^{\frac{1}{2}+\delta} \left(\sum_{i=1}^N \|\lambda_i\|_{\delta,\gamma_i}^2 \right)^{\frac{1}{2}} \right).$$

Proof. First, using standard interpolation estimates (see [10]), and $\tilde{h} \leq h$, we obtain

$$(3.6) \quad \|(\eta^u, \eta^\lambda)\|_{W_h} \leq C \left(h^s |u|_{1+s,\Omega} + h^{\frac{1}{2}+\delta} \left(\sum_{i=1}^N \|\lambda_i\|_{\delta,\gamma_i}^2 \right)^{\frac{1}{2}} \right).$$

To bound the discrete error, we first suppose that $s > \frac{1}{2}$. Then, using Theorem 2.1 and Lemma 2.1, we arrive at

$$(3.7) \quad \begin{aligned} \|(e_h^u, e_h^\lambda)\|_{W_h}^2 &= B((e_h^u, e_h^\lambda), (e_h^u, -e_h^\lambda)) = B((\eta^u, \eta^\lambda), (e_h^u, -e_h^\lambda)) \\ &= (\nabla \eta^u, \nabla e_h^u)_\Omega - \sum_{i=1}^N \langle \eta^{\lambda_i}, e_h^u \rangle_{\gamma_i} + \sum_{i=1}^N \langle e_h^{\lambda_i}, \eta^u \rangle_{\gamma_i} + \sum_{i=1}^N h \langle -\eta^{\lambda_i}, -e_h^{\lambda_i} \rangle_{\gamma_i} \\ &= I + II + III + IV. \end{aligned}$$

We now bound the above right-hand side term by term. The main arguments are the approximation properties of i_h and $\Pi_{\tilde{h}}$ (see [10]), the duality between $H^{-\frac{1}{2}}(\gamma_i)$ and $H^{\frac{1}{2}}(\gamma_i)$, the Trace Theorem in each B_i , the local trace result from Lemma 3.1, and the Cauchy-Schwarz and Poincaré inequalities:

$$(3.8) \quad I \leq |\eta^u|_{1,\Omega} |e_h^u|_{1,\Omega} \leq Ch^{2s} |u|_{1+s,\Omega}^2 + \frac{1}{4} |e_h^u|_{1,\Omega}^2,$$

$$(3.9) \quad II \leq \sum_{i=1}^N \|\eta^{\lambda_i}\|_{-\frac{1}{2},\gamma_i} \|e_h^u\|_{\frac{1}{2},\gamma_i} \leq \sum_{i=1}^N \|\eta^{\lambda_i}\|_{-\frac{1}{2},\gamma_i} \|e_h^u\|_{1,B_i} \leq C \sum_{i=1}^N h^{1+2\delta} \|\lambda_i\|_{\delta,\gamma_i}^2 + \frac{1}{4} |e_h^u|_{1,\Omega}^2,$$

$$\begin{aligned}
(3.10) \quad III &\leq \frac{1}{4} \sum_{i=1}^N h \|e_h^{\lambda_i}\|_{0,\gamma_i}^2 + \sum_{i=1}^N h^{-1} \|\eta^u\|_{0,\gamma_i}^2 \\
&\leq \frac{1}{4} \sum_{i=1}^N h \|e_h^{\lambda_i}\|_{0,\gamma_i}^2 + \sum_{i=1}^N 8 \left(h^{-2} \|\eta^u\|_{0,\tilde{B}_i}^2 + h^{-1} \|\eta^u\|_{0,\tilde{B}_i} \|\nabla \eta^u\|_{0,\tilde{B}_i} \right) \\
&\leq \frac{1}{4} \sum_{i=1}^N h \|e_h^{\lambda_i}\|_{0,\gamma_i}^2 + CMh^{2s} |u|_{1+s,\Omega}^2,
\end{aligned}$$

$$(3.11) \quad IV \leq \sum_{i=1}^N h \|\eta^{\lambda_i}\|_{0,\gamma_i}^2 + \frac{1}{4} \sum_{i=1}^N h \|e_h^{\lambda_i}\|_{0,\gamma_i}^2 \leq C \sum_{i=1}^N h^{1+2\delta} \|\lambda_i\|_{\delta,\gamma_i}^2 + \frac{1}{4} \sum_{i=1}^N h \|e_h^{\lambda_i}\|_{0,\gamma_i}^2.$$

Collecting then (3.7)-(3.11), we get

$$\|(e_h^u, e_h^\lambda)\|_{W_h}^2 \leq C \left((1+M)h^{2s} |u|_{1+s,\Omega}^2 + h^{1+2\delta} \sum_{i=1}^N \|\lambda_i\|_{\delta,\gamma_i}^2 \right) + \frac{1}{2} \|(e_h^u, e_h^\lambda)\|_{W_h}^2,$$

and (3.5) follows by rearranging terms and applying the triangle inequality and (3.6). Next, if $s \leq \frac{1}{2}$, proceeding as above, we get

$$\|(e_h^u, e_h^\lambda)\|_{W_h}^2 = I + II + III + IV + \sum_{i=1}^N h \langle \lambda_i, e_h^{\lambda_i} \rangle_{\gamma_i}.$$

The first four terms have already been bounded. The fifth is bounded as follows:

$$\sum_{i=1}^N h \langle \lambda_i, e_h^{\lambda_i} \rangle_{\gamma_i} \leq \sum_{i=1}^N h \|\lambda_i\|_{0,\gamma_i} \|e_h^{\lambda_i}\|_{0,\gamma_i} \leq \sum_{i=1}^N h \|\lambda_i\|_{0,\gamma_i}^2 + \frac{1}{4} \sum_{i=1}^N h \|e_h^{\lambda_i}\|_{0,\gamma_i}^2.$$

Then (3.5) follows rearranging terms, and applying the triangle inequality and (3.6). \square

Remark 3.2. *The proof of the last result does not depend explicitly on N , the number of perforations. It does, nevertheless, show a mild dependence on M (defined in (3.2)). In fact, the error constant grows with \sqrt{M} , due to the bound on the term III above. This fact makes the estimates of interest when the value M does not blow up. This means that, for a given mesh, the number of inclusions can not grow in an unbounded way (since M would go to infinity). On the other hand, if only a few inclusions are present in the domain, then the constant M will remain moderate even for coarse meshes. It is important to remark that this problem is of no importance once the mesh is refined enough, since the annular regions \tilde{B}_i become more and more separated (hence, in practice, reducing M), but this might be an issue when the mesh is coarse.*

One further important point on the error estimate lies in the regularity of the solution of (1.2). Since the inclusions B_i are supposed to be smooth, then, if Ω is supposed to be convex and g_i are smooth enough, it is easy to see that $u \in H^2(\omega)$ and $u \in H^2(B_i)$ for each $i = 1, \dots, N$. In this case, $\lambda_i \in H^{\frac{1}{2}}(\gamma_i)$ for each $i = 1, \dots, N$. Concerning the regularity of u in the whole of Ω , as it was mentioned in the introduction, u belongs at least to $H^{\frac{3}{2}-\varepsilon}(\Omega)$ for any $\varepsilon > 0$ (see [13] for a discussion).

One final important factor on (3.5) is the behavior of the norms of the exact solution on the right-hand side of the error estimate. As a matter of fact, the behavior of the norm of the solution u can vary dramatically according to the distribution of the inclusions B_i . If the inclusions get closer together, then the problem tends to be a partial differential equation posed on a non-Lipschitz domain, in which case the regularity of u changes significantly, and then the

norm on the right-hand side of (3.5) blows up as the distance between inclusions gets smaller. Moreover, even if the inclusions B_i are separated, the distance between them affects the norm of the solution u . In fact, it is easy to see that the norm of u depends on some negative power of the distance between the inclusions. Hence, we do not expect the present approach to provide error estimates which do not depend on the number of inclusions, or in the distance between them. On the other hand, the numerical results show a reasonably robust behavior of the error with respect to the distance between the inclusions, especially on the far field.

Remark 3.3. It is worth remarking that the method can be written in a completely consistent way, at least in the case in which all the γ_i are curved boundaries. As a matter of fact, in such a case we have $[[\partial_{\mathbf{n}}v_h]]_{\gamma_i} = 0$ for all $v_h \in V_h$ and all $i = 1, \dots, N$ (see Figure 2 for a typical situation, as can be seen there, ∇v_h is the same constant both sides of the curve γ_i , at almost every point of it). Then the bilinear form \mathbf{B} can be rewritten as

$$(3.12) \quad \mathbf{B}((u_h, \boldsymbol{\lambda}_{\tilde{h}}), (v_h, \boldsymbol{\mu}_{\tilde{h}})) = (\nabla u_h, \nabla v_h)_{\Omega} - \sum_{i=1}^N \langle \lambda_{i, \tilde{h}}, v_h \rangle_{\gamma_i} - \sum_{i=1}^N \langle \mu_{i, \tilde{h}}, u_h \rangle_{\gamma_i} \\ + \sum_{i=1}^N h \langle [[\partial_{\mathbf{n}}u_h]] - \lambda_{i, \tilde{h}}, [[\partial_{\mathbf{n}}v_h]] + \mu_{i, \tilde{h}} \rangle_{\gamma_i},$$

and then (2.3) follows using $\lambda_i - [[\partial_{\mathbf{n}}u]]_{\gamma_i} = 0$ for all $i = 1, \dots, N$. Looking at this last writing the link to the Barbosa-Hughes method (and the method from [16]) is apparent. Nevertheless, we have preferred to keep the non-consistent presentation here since the definition (3.12) leads to technical difficulties. More precisely, for this alternative writing of \mathbf{B} Lemma 3.1 would have to be applied with respect to the interior of B_i , which would lead, ultimately, to error estimates that depend on $\text{diam}(B_i)^{-1}$.

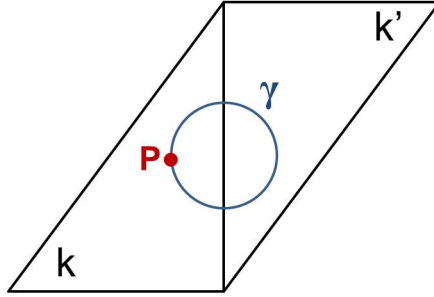


FIGURE 2. A typical situation in which the inclusion B_i is a circle.

4. NUMERICAL STUDIES

In this section we report the results of numerical experiments that support the analysis carried out in the previous sections. All computations have been performed using a code written in *FreeFem++* [17].

For the first test case we consider the stabilised problem (2.1) with $\omega = \Omega \setminus \cup_{i=1}^3 B_i$, where $\Omega = (0, 10)^2$, and $B_i = B[\mathbf{c}_i, r]$, where $r > 0$. The centers of the balls B_i are $\mathbf{c}_1 = (1.7, 7.4)$, $\mathbf{c}_2 = (5.7, 8.4)$, and $\mathbf{c}_3 = (8.7, 3.4)$, respectively. To build the meshes a parameter n is given. Then Ω is divided horizontally and vertically into $10n$ segments. The mesh on each γ_i is built by dividing each one of them into $8n$ curved segments. A zoom around B_1 of the resulting mesh

when $n = 1$ and $r = 0.1$ is depicted in Figure 3, where we can observe that the finite element mesh does not resolve the geometrical feature that is B_1 . More importantly, for all the values of n , the mesh parameters satisfy $|\tilde{e}| < h$, and then stabilisation is indeed needed.

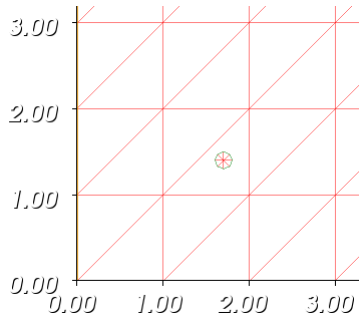


FIGURE 3. A zoom of the computational mesh in a neighborhood of B_1 for $r = 0.1$ and $n = 1$. We can observe that the mesh does not resolve the inclusion.

We first test the method on an example with a smooth analytical solution. We set the right-hand side f and the boundary conditions in such a way that the exact solution is given by

$$u(x, y) = \sin(x) \sin(y) \quad \text{in } \Omega.$$

In Table 1 we report the results for this test case when $r = 0.1$, while in Table 2 we consider $r = 0.025$ (qualitatively similar results have been obtained for other choices of r , so we only report these for brevity). We observe that, since $u \in H^2(\Omega)$ and $\boldsymbol{\lambda} = \mathbf{0}$, then the optimal order of convergence $O(h)$ is obtained, with an even better than optimal convergence for $\boldsymbol{\lambda}$. This is most likely due to the fact $\boldsymbol{\lambda} = \mathbf{0}$, and is coherent with the results obtained in [3].

We next move onto a case in which the exact solution is not known. More precisely, we consider the approximation of the following boundary value problem:

$$(4.1) \quad \begin{aligned} -\Delta u &= 0 \quad \text{in } \omega, \\ u &= 10 \quad \text{on } \gamma_i, i = 1, 2, 3, \quad u = 0 \quad \text{on } \partial\Omega. \end{aligned}$$

To estimate the error committed by the present method, we have computed a reference solution using a standard finite element method in ω using a mesh containing 71,200 \mathbb{P}_2 elements. We denote this solution by u_{ref} . The reference solution is depicted in Figure 4 (top). For the fictitious domain computations we have extended the function \tilde{f} by zero to $\Omega \setminus \omega$. On the bottom of Figure 4 we depict the discrete solution obtained using $n = 10$. Moreover, in Figure 5 we depict cross-sections of the different approximations to u along the line $y = 8.4$. We can see the discrete solution approaches the reference one as the mesh gets refined, recovering an accurate far field profile from early on (of course, since the boundary conditions on γ_i are imposed weakly, we can not expect these to be well reproduced by the discrete solution, unless the mesh is extremely refined). To make these results more precise, we have computed the errors $\|u_{\text{ref}} - u_h\|_{0,\omega}$ and $\|u_{\text{ref}} - u_h\|_{1,\omega}$ for different values of n , and report them in Table 3 for $r = 0.2$, and in Table 4 for $r = 0.025$ (again, qualitatively similar results have been obtained for other radii, we only report these ones for brevity). We see the errors approach zero, but with a slower rate. This is in accordance with the fact that the exact solution of the fictitious domain problem does not belong to $H^2(\Omega)$, and the fact that, since $h > \text{diam}(B_i)$, these results still show a pre-asymptotic regime.

n	$\ u - u_h\ _{1,\Omega}$	order	$\left(\sum_{i=1}^3 h\ \lambda - \lambda_h\ _{0,\gamma_i}^2\right)^{\frac{1}{2}}$	order
1	3.5800		0.1986	
2	1.7993	0.99	0.0595	1.73
3	1.1986	1.00	0.0256	2.08
4	0.8989	1.00	0.0156	1.72
8	0.4489	1.00	0.0038	2.03
12	0.3001	0.99	0.0020	1.58
16	0.2244	1.00	0.0011	2.07

TABLE 1. Finite element errors for the smooth example and $r = 0.1$.

n	$\ u - u_h\ _{1,\Omega}$	order	$\left(\sum_{i=1}^3 h\ \lambda - \lambda_h\ _{0,\gamma_i}^2\right)^{\frac{1}{2}}$	order
1	3.5804		0.1088	
2	1.7993	0.99	0.0384	1.50
3	1.1986	1.00	0.0152	2.28
4	0.8988	1.00	0.0124	0.70
8	0.4489	1.00	0.0033	1.90
12	0.3001	0.99	0.0015	1.94
16	0.2243	1.01	0.0008	2.18

TABLE 2. Finite element errors for the smooth example and $r = 0.025$.

n	$\ u_{\text{ref}} - u_h\ _{0,\omega}$	order	$\ u_{\text{ref}} - u_h\ _{1,\omega}$	order
1	17.9261		28.069	
2	12.4341	0.52	20.0713	0.48
3	9.5128	0.66	15.7798	0.59
4	7.9418	0.62	13.0286	0.66
8	4.5119	0.81	7.9581	0.71
12	3.1452	0.88	5.9118	0.73
16	2.3856	0.96	4.7040	0.79

TABLE 3. Errors $\|u_{\text{ref}} - u_h\|_{0,\omega}$ and $\|u_{\text{ref}} - u_h\|_{1,\Omega}$ for $r = 0.2$.

n	$\ u_{\text{ref}} - u_h\ _{0,\omega}$	order	$\ u_{\text{ref}} - u_h\ _{1,\omega}$	order
1	14.8711		24.4094	
2	13.1243	0.18	22.3855	0.12
3	11.8203	0.25	20.2568	0.24
4	10.5745	0.38	18.9668	0.22
8	7.4988	0.49	14.536	0.38
12	5.8831	0.59	11.7656	0.52
16	4.9088	0.62	9.8383	0.62

TABLE 4. Errors $\|u_{\text{ref}} - u_h\|_{0,\omega}$ and $\|u_{\text{ref}} - u_h\|_{1,\Omega}$ for $r = 0.025$.

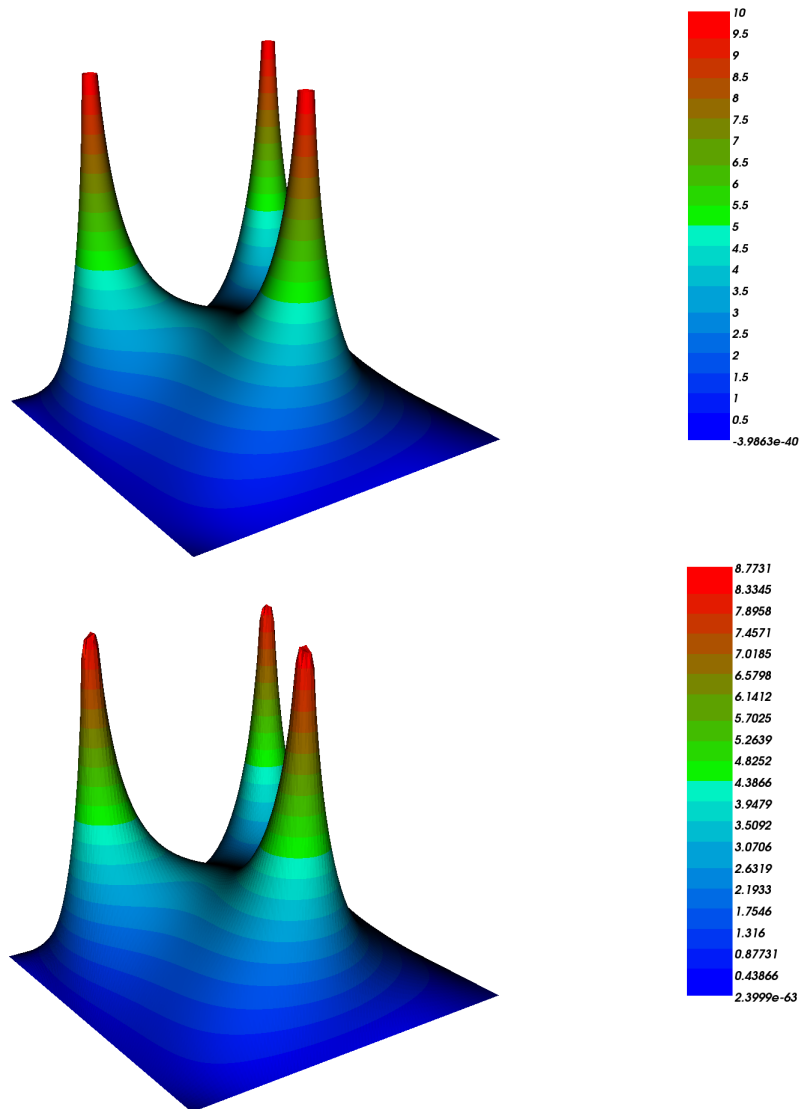


FIGURE 4. Reference solution u_{ref} (top) and approximate solution u_h for $n = 10$, for $r = 0.2$.

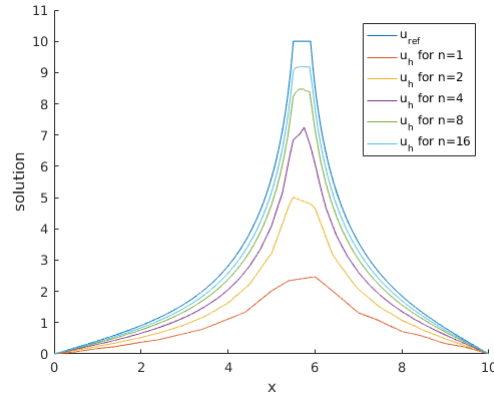


FIGURE 5. Cross-section of the solution for different values of n along the line $y = 8.4$.

We now present a second set of numerical experiments whose goal is twofold. First, we will try to assess how the error behaves in the case the domain contains more inclusions than in the previous case, and how it behaves when the inclusions get closer together. Also, we will measure the error in region that does not intersect the inclusions (i.e., in the "far field" region). For this we consider $\omega = \Omega \setminus \cup_{i=1}^9 B_i$, where $\Omega = (0, 10)^2$ and the B_i 's are the circles with radius 0.1. These circles' centers are given in Table 5. We can see that the distances between circles varies significantly. The boundary value problem solved is the following:

$$(4.2) \quad \begin{aligned} -\Delta u &= 0 && \text{in } \omega, \\ u &= 6 && \text{on } \gamma_1, \gamma_4 \text{ and } \gamma_7, \\ u &= 8 && \text{on } \gamma_2, \gamma_5 \text{ and } \gamma_8, \\ u &= 10 && \text{on } \gamma_3, \gamma_6 \text{ and } \gamma_9, \\ u &= 0 && \text{on } \partial\Omega. \end{aligned}$$

	B_1	B_2	B_3	B_4	B_5	B_6	B_7	B_8	B_9
CASE 1	(6.6, 9.2)	(7.8, 9.2)	(9, 9.2)	(6.6, 8)	(7.8, 8)	(9, 8)	(6.6, 6.8)	(7.8, 6.8)	(9, 6.8)
CASE 2	(7.6, 9.2)	(8.3, 9.2)	(9, 9.2)	(7.6, 8.5)	(8.3, 8.5)	(9, 8.5)	(7.6, 7.8)	(8.3, 7.8)	(9, 7.8)
CASE 3	(8.4, 9.2)	(8.7, 9.2)	(9, 9.2)	(8.4, 8.9)	(8.7, 8.9)	(9, 8.9)	(8.4, 8.6)	(8.7, 8.6)	(9, 8.6)

TABLE 5. Centers of the inclusions B_i . The distance between the inclusions gets smaller from CASE 1 to CASE 3.

Once again, a reference solution using quadratic elements in a highly refined mesh has been obtained for each case, and the errors have been computed with respect to it. The meshes used to solve the stabilised problem (2.1) have been generated in the same way as for the previous example. For the Case 2, the reference solution to this problem is depicted in Fig. 6, and cross sections of different approximations of u are depicted in Fig. 7. We have measured the norms in $L^2(\omega)$ and $H^1(\omega)$ of the error, as well as the norms $\|u_{\text{ref}} - u_h\|_{0, \tilde{\Omega}}$ and $\|u_{\text{ref}} - u_h\|_{1, \tilde{\Omega}}$, where $\tilde{\Omega} = (0, 5)^2$. The latter aims at assessing how the error behaves in the far field. The results for the three cases are reported in Tables 6-8. Finally, to assess the robustness of the method with respect to the number of inclusions, we have repeated the same test case but considering only 3 inclusions. We have kept only the circles B_1, B_2 and B_3 with $u = 6, 8, 10$ in $\gamma_1, \gamma_2, \gamma_3$,

respectively. We report the results for Case 3 only, as similar results have been obtained for other distances. The errors are reported in Table 9. Two main conclusions can be drawn from these results. First, the size of the errors does not seem to be affected by the number of inclusions, and the distance between them. Also, close to optimal $L^2(\tilde{\Omega})$ results can be observed, while the convergence rate in the $H^1(\tilde{\Omega})$ norm does not seem to be significantly better than in the whole of ω (although, as expected, the errors themselves are significantly smaller). On the other hand, when we have reduced the number of inclusions, the results in Table 9 show, once again, that the errors themselves do not seem to be very affected by this, but show a slightly better behavior as far as the convergence rate in the H^1 norms is concerned. This indicates the presence of a larger pre-asymptotic regime in the case more inclusions are present, and when they are packed closer together.

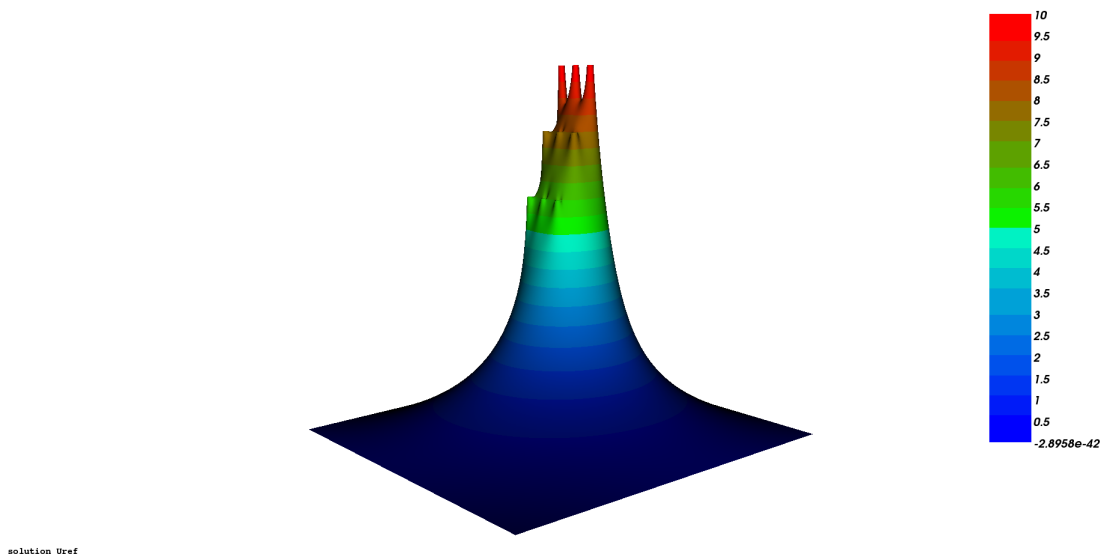


FIGURE 6. Reference solution u_{ref} for CASE 2.

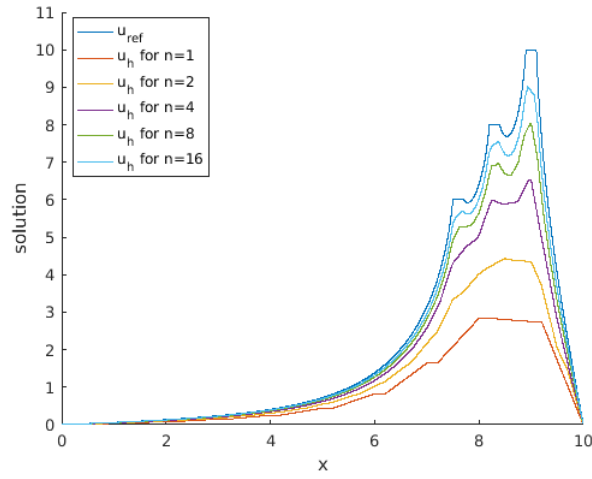


FIGURE 7. Cross-sections of u_{ref} and u_h at $y = 9.2$ for different values of n for CASE 2.

	$\ u_{\text{ref}} - u_h\ _{0,\omega}$	order	$\ u_{\text{ref}} - u_h\ _{1,\omega}$	order
$n = 1$	14.782		24.374	
$n = 2$	9.7017	0.60	18.4522	0.40
$n = 3$	7.2801	0.70	14.9537	0.51
$n = 4$	5.9660	0.69	12.447	0.63
$n = 8$	3.3513	0.83	8.1707	0.60
$n = 12$	2.3579	0.86	6.1067	0.71
$n = 16$	1.7774	0.98	5.0732	0.64
	$\ u_{\text{ref}} - u_h\ _{0,\tilde{\Omega}}$	order	$\ u_{\text{ref}} - u_h\ _{1,\tilde{\Omega}}$	order
$n = 1$	1.5405		1.7353	
$n = 2$	0.9367	0.71	1.0551	0.71
$n = 3$	0.6774	0.79	0.7628	0.80
$n = 4$	0.5453	0.75	0.6139	0.75
$n = 8$	0.2938	0.89	0.3306	0.89
$n = 12$	0.1998	0.95	0.2249	0.95
$n = 16$	0.1514	0.96	0.1703	0.96

TABLE 6. Numerical results for 9 inclusions. Case 1.

	$\ u_{\text{ref}} - u_h\ _{0,\omega}$	order	$\ u_{\text{ref}} - u_h\ _{1,\omega}$	order
$n = 1$	10.0212		19.0608	
$n = 2$	6.3462	0.65	14.4058	0.40
$n = 3$	4.6790	0.75	11.7454	0.50
$n = 4$	3.8471	0.68	9.7236	0.65
$n = 8$	2.1402	0.84	6.5995	0.55
$n = 12$	1.5151	0.85	5.0054	0.68
$n = 16$	1.1449	0.97	4.2300	0.58
	$\ u_{\text{ref}} - u_h\ _{0,\tilde{\Omega}}$	order	$\ u_{\text{ref}} - u_h\ _{1,\tilde{\Omega}}$	order
$n = 1$	0.6694		0.7564	
$n = 2$	0.4111	0.70	0.4642	0.70
$n = 3$	0.2978	0.79	0.3362	0.79
$n = 4$	0.2440	0.69	0.2752	0.69
$n = 8$	0.1331	0.87	0.1500	0.87
$n = 12$	0.0923	0.90	0.1040	0.90
$n = 16$	0.0706	0.93	0.0796	0.92

TABLE 7. Numerical results for 9 inclusions. Case 2.

	$\ u_{\text{ref}} - u_h\ _{0,\omega}$	order	$\ u_{\text{ref}} - u_h\ _{1,\omega}$	order
$n = 1$	5.2804		14.8082	
$n = 2$	3.3580	0.65	11.6816	0.34
$n = 3$	2.6033	0.62	9.8871	0.41
$n = 4$	2.1365	0.68	8.8501	0.38
$n = 8$	1.2823	0.73	6.679	0.40
$n = 12$	0.9562	0.72	5.4516	0.50
$n = 16$	0.7457	0.86	4.8062	0.43
	$\ u_{\text{ref}} - u_h\ _{0,\tilde{\Omega}}$	order	$\ u_{\text{ref}} - u_h\ _{1,\tilde{\Omega}}$	order
$n = 1$	0.1964		0.2253	
$n = 2$	0.1428	0.45	0.1623	0.47
$n = 3$	0.1165	0.50	0.1318	0.51
$n = 4$	0.0958	0.68	0.1082	0.68
$n = 8$	0.0594	0.69	0.0669	0.69
$n = 12$	0.0445	0.71	0.0502	0.70
$n = 16$	0.0356	0.77	0.0401	0.78

TABLE 8. Numerical results for 9 inclusions. Case 3.

	$\ u_{\text{ref}} - u_h\ _{0,\omega}$	order	$\ u_{\text{ref}} - u_h\ _{1,\omega}$	order
$n = 1$	5.7001		15.1578	
$n = 2$	3.8427	0.56	12.1899	0.31
$n = 3$	2.9783	0.62	10.036	0.47
$n = 4$	2.5517	0.53	8.4937	0.58
$n = 8$	1.5315	0.73	5.9490	0.51
$n = 12$	1.0832	0.85	4.7315	0.56
$n = 16$	0.8446	0.86	4.0229	0.56
	$\ u_{\text{ref}} - u_h\ _{0,\tilde{\Omega}}$	order	$\ u_{\text{ref}} - u_h\ _{1,\tilde{\Omega}}$	order
$n = 1$	0.2497		0.2808	
$n = 2$	0.1686	0.56	0.1895	0.56
$n = 3$	0.1354	0.54	0.1521	0.54
$n = 4$	0.1175	0.49	0.1320	0.49
$n = 8$	0.0711	0.72	0.0799	0.72
$n = 12$	0.0494	0.89	0.0555	0.89
$n = 16$	0.0388	0.83	0.0436	0.83

TABLE 9. Numerical results for 3 inclusions. These inclusions are B_1, B_2 and B_3 from Case 3.

5. CONCLUSION

In this work we have proposed a simple stabilised finite element method to approximate the solution of partial differential equations posed in domains containing a moderate amount of small perforations. The method is a fictitious domain method, enhanced with a stabilisation term that, in some cases, is reminiscent of the Barbosa-Hughes stabilised method. The numerical results show that, at least for the cases presented in this work, this method can be used to approximate the solution (especially the far field) with a good accuracy, without the need to modify the finite element space, or to consider especial geometries. We do not expect this method to give accurate results if we consider a domain with a very large number of perforations. But, as long as this number remains moderate, we believe the present approach presents a simple alternative to previously existing references. This claim is supported by our numerical experiments, that show that the method behaves in a robust way with respect to the number of inclusions, and the distance between them. There are, nevertheless, several questions that remain open. One is the possibility of performing a local error analysis. The numerical results show that the error is not optimal (i.e., $O(h)$) in the H^1 norm of a subset of ω far away from the inclusions, but it is nevertheless better than the convergence in the whole of ω . Another possibility for future research is exploring the coupling of this method with the smooth extension method proposed in [11], since that method proposes a way to extend the solution \tilde{u} to an $H^2(\Omega)$ function. Then, Theorem 3.1 would provide an $O(h)$ convergence for the stabilised method, and optimal convergence of the full scheme could be reached. Another problem that remains open is the application of this strategy to problems in fluid mechanics. In this case, the same approach can be followed, and the Lagrange multiplier represents the jump of the Cauchy stress tensor (see, e.g., [9] for a method based on the XFEM idea). There, especial consideration should be paid to issues such as mass conservation on the original (perforated) domain. These topics will be the subject of future research.

Acknowledgments : A part of this work was carried out during the visit of GRB to the Hausdorff Research Institute for Mathematics, Bonn, in the framework of the trimester program *Multiscale Problems: Algorithms, Numerical Analysis and Computation*, during March 2017.

REFERENCES

- [1] P. Antonietti, A. Cangiani, J. Collis, Z. Dong, E. Georgoulis, S. Giani, and P. Houston. Review of discontinuous Galerkin finite element methods for partial differential equations on complicated domains. In *Building bridges, connections and challenges in modern approaches to numerical partial differential equations. Lecture Notes in Computational Science and Engineering, Vol. 114*, pages 279–308. Springer, Heidelberg, 2016.
- [2] H. J. C. Barbosa and T. J. R. Hughes. The finite element method with Lagrange multipliers on the boundary: circumventing the Babuška-Brezzi condition. *Comput. Methods Appl. Mech. Engrg.*, 85(1):109–128, 1991.
- [3] G. R. Barrenechea and F. Chouly. A local projection stabilized method for fictitious domains. *Appl. Math. Lett.*, 25(12):2071–2076, 2012.
- [4] S. Bertoluzza, M. Ismail, and B. Maury. Analysis of the fully discrete fat boundary method. *Numer. Math.*, 118(1):49–77, 2011.
- [5] E. Burman and P. Hansbo. Fictitious domain finite element methods using cut elements: I. A stabilized Lagrange multiplier method. *Comput. Methods Appl. Mech. Engrg.*, 199(41-44):2680–2686, 2010.
- [6] E. Burman and P. Hansbo. Fictitious domain finite element methods using cut elements: II. A stabilized Nitsche method. *Appl. Numer. Math.*, 62(4):328–341, 2012.
- [7] A. Cangiani, E. H. Georgoulis, and P. Houston. *hp*-version discontinuous Galerkin methods on polygonal and polyhedral meshes. *Math. Models Methods Appl. Sci.*, 24(10):2009–2041, 2014.
- [8] A. Cangiani, E. H. Georgoulis, and Y. Sabawi. Adaptive discontinuous Galerkin methods for elliptic interface problems. 2016. Submitted for publication.
- [9] S. Court, M. Fournié, and A. Lozinski. A fictitious domain approach for the Stokes problem based on the extended finite element method. *Internat. J. Numer. Methods Fluids*, 74(2):73–99, 2014.
- [10] A. Ern and J.-L. Guermond. *Theory and Practice of Finite Elements*, volume 159 of *Applied Mathematical Sciences*. Springer-Verlag, New York, 2004.
- [11] B. Fabrèges, L. Gouarin, and B. Maury. A smooth extension method. *C. R. Math. Acad. Sci. Paris*, 351(9-10):361–366, 2013.
- [12] S. Giani and P. Houston. *hp*-adaptive composite discontinuous Galerkin methods for elliptic problems on complicated domains. *Numer. Methods Partial Differential Equations*, 30(4):1342–1367, 2014.
- [13] V. Girault and R. Glowinski. Error analysis of a fictitious domain method applied to a Dirichlet problem. *Japan J. Indust. Appl. Math.*, 12(3):487–514, 1995.
- [14] R. Glowinski, T.-W. Pan, and J. Périaux. A fictitious domain method for Dirichlet problem and applications. *Comput. Methods Appl. Mech. Engrg.*, 111(3-4):283–303, 1994.
- [15] W. Hackbusch and S. A. Sauter. Composite finite elements for the approximation of PDEs on domains with complicated micro-structures. *Numer. Math.*, 75(4):447–472, 1997.
- [16] J. Haslinger and Y. Renard. A new fictitious domain approach inspired by the extended finite element method. *SIAM J. Numer. Anal.*, 47(2):1474–1499, 2009.
- [17] F. Hecht. New development in freefem++. *J. Numer. Math.*, 20(3-4):251–265, 2012.
- [18] C. Le Bris, F. Legoll, and A. Lozinski. An MsFEM type approach for perforated domains. *Multiscale Model. Simul.*, 12(3):1046–1077, 2014.
- [19] B. Maury. A fat boundary method for the Poisson problem in a domain with holes. *J. Sci. Comput.*, 16(3):319–339, 2001.
- [20] N. Moës, E. Béchet, and M. Tourbier. Imposing Dirichlet boundary conditions in the extended finite element method. *Internat. J. Numer. Methods Engrg.*, 67(12):1641–1669, 2006.
- [21] D. Peterseim and S. A. Sauter. The composite mini element-coarse mesh computation of Stokes flows on complicated domains. *SIAM J. Numer. Anal.*, 46(6):3181–3206, 2008.
- [22] I. Ramière. Convergence analysis of the Q_1 -finite element method for elliptic problems with non-boundary-fitted meshes. *Internat. J. Numer. Methods Engrg.*, 75(9):1007–1052, 2008.

(G.R.B.) DEPARTMENT OF MATHEMATICS AND STATISTICS, UNIVERSITY OF STRATHCLYDE, 26 RICHMOND STREET, GLASGOW G1 1XH, SCOTLAND. gabriel.barrenechea@strath.ac.uk

(C.G.) DEPARTMENT OF MATHEMATICS AND STATISTICS, UNIVERSITY OF STRATHCLYDE, 26 RICHMOND STREET, GLASGOW G1 1XH, SCOTLAND. cheherazada.gonzalez@strath.ac.uk